Astron. Astrophys. 356, 643–653 (2000)

ASTRONOMY AND ASTROPHYSICS

Multiperiodic light variations of active stars

K. Oláh[1], **Z. Kolláth**[1], **and K.G. Strassmeier**[2]

[1] Konkoly Observatory of the Hungarian Academy of Sciences, 1525 Budapest, Hungary (olah@konkoly.hu, kollath@konkoly.hu)
[2] Institute for Astronomy, University of Vienna, Türkenschanzstrasse 17, 1180 Vienna, Austria (strassmeier@astro.univie.ac.at)

Received 2 November 1999 / Accepted 5 January 2000

Abstract. We studied the long-term light behaviour of ten rapidly-rotating active stars (LQ Hya, V833 Tau, EI Eri, V711 Tau, BY Dra, HU Vir, IL Hya, VY Ari, HK Lac, IM Peg) with Fourier analysis. Using photometric databases of up to 30 years in length, we search for periodic or quasi-periodic long-term variations of the overall light levels. Out of the ten stars studied, nine show cyclic variability and six of those seem to vary on two or multiple time-scales. Using additional data from the literature, we found that cycle lengths were generally longer for stars with longer rotation periods. The inverse Rossby numbers of these stars show a correlation with $\omega_{cyc}/\Omega(=P_{rot}/P_{cyc})$ calculated from the shortest cycle length. The cycle lengths of several stars agree well with other types of cycles determined earlier.

Using artificial test data, we found that the cyclic variation of the average light level is determined by the change in the spot/plage coverage alone and that spot migration does not play a significant role in the shape or length of the long-term brightness changes.

Key words: stars: activity – stars: binaries: close – stars: late-type – stars: rotation – stars: starspots – techniques: photometric

1. Introduction

The long-term photometric variability of spotted binary stars was first documented by Phillips & Hartmann (1978) from their combination of photographic magnitudes from archival plate collections and new photoelectric measurements. They found a 50–60 years long variation for BY Dra and CC Eri. A similar result was published shortly thereafter by Hartmann et al. (1981) for V833 Tau and was confirmed by Bondar (1995). The accuracy of the photographic measurements was usually no better than $\pm 0\overset{\mathrm{m}}{.}1$, and sometimes even worse, and created the need of long-term photoelectric monitoring of spotted stars.

However, because of the relatively short time-base of the more accurate photoelectric observations, it was not possible to find well-determined cycles in that measures alone. Nevertheless, 'cycles' were searched for and possibly found for a few very active systems (see, e.g., Strassmeier et al. 1997 and references therein), but the cycle periods were either resembling the solar value or were similar to the length of the given database. Another problem is that, depending on the inclination of the rotational axis, the rotational modulation could dominate over the long-term changes. In these cases only very precise observations would show clearly the long-term modulation of the light variability and, at the same time, would allow a search for even multiperiodic variations. The existence of several solar activity cycles amply demonstrates such multiperiodic behaviour for the Sun (e.g. Sonett et al. 1991). Our aim in this paper is thus to find such multiperiodic behaviour on other stars and establish possible correlations between cycle lengths and other characteristic stellar parameters.

The most well-known attempt to find correlations between the lengths of activity cycles and other physical parameters is the Mt Wilson Ca II H&K survey of solar-like stars started by Wilson back in 1966 (e.g. Wilson 1978). As the chromospheric H&K database is continuously growing, that program is the source of more and more results, both observationally and theoretically. In the past years it was extended to photometric observations of the stellar photospheres (see Radick et al. 1998 and references therein). Recent advances from this program include the establishment of an empirical connection of the observed H&K cycle lengths to dynamo theory (Baliunas et al. 1996).

Other methods also led to the discovery of possible activity cycles of active stars. Massi et al. (1998) used radio observations of the RS CVn system UX Ari and derived two short-term cycles of 25.5 and 158 days in the (radio) activity level. Berdyugina & Tuominen (1998) found active longitudes and cycles in four RS CVn systems from phase changes of the two minima of the spotted light curves. On the Sun, Pulkkinen et al. (1999) found a 90 years long cycle using north-south asymmetries of sunspots which length is closely resembling the Gleissberg cycle. Note though that the last two approaches found periodicities mainly in the spot pattern rather than in the overall activity level. It is another goal of this paper to establish first relations between the various types of stellar cycles.

In this paper, we focus on ten well-studied rapidly-rotating active stars. All except one are components of RS CVn-type binary systems. One of the most comprehensive, and also precise, photoelectric datasets to date was recently published by Strass-

Send offprint requests to: K. Oláh

meier et al. (1997, hereafter SBCR) for 23 active stars. One of their intentions was to build up a database for studying long-term variabilities of the program stars. They compiled all the data from the literature and added 9,250 new UBVRI data from seven years of monitoring with automated telescopes in Arizona and Sicily. Using this dataset, Oláh & Kolláth (1999) conducted a preliminary Fourier analysis for nine of the ten active stars in this paper, and already suggested that cycle lengths were longer for stars with longer rotational periods. In the present work, we carry out a much more detailed analysis of these nine (plus one additional) stars and supplement the dataset of SBCR by three additional years (1997–1999) of continuous photoelectric photometry from the two Vienna automatic photoelectric telescopes (APTs).

2. Description and test of the method

2.1. Low-frequency Fourier analysis

Throughout this paper, we applied the multifrequency analysis program MUFRAN (Kolláth 1990), which is a collection of methods for analysing multiperiodic, unevenly sampled data. Standard discrete Fourier transforms (DFT) of the light-curves were calculated, followed by a non-linear least-square fit of the frequencies found.

We prefer to use standard Fourier transformation together with consecutive prewhitening by a least-square Fourier fit to the light-curve data. Thorough application of this method guarantees that no suspicious periodicities are introduced during the analysis if we use only a few (2-3) Fourier components. Automatic methods for frequency search (like the CLEAN algorithm, Roberts et al. 1984) could force non-existing periodicities to be included in the fit. We also note that for multiperiodic signals with no strong harmonic structure the standard Fourier transform performs better than phase-dispersion methods.

We only searched for periods or quasi-periods that were at least an order of magnitude longer than the rotational periods. Years or decades long variations are seen in the datasets and some of them were modulated with an even longer-term variability. We consecutively removed the lower frequencies from the datasets until a white-noise spectrum remained. In extreme cases the longest variations detectable seemed to be longer than the length of the datasets themselves and then we adopted trends to remove them from the data. These long periods were used only as tools; fits with two closely spaced periods could equally well remove the long-term trend from the data. The resulting periods after removal of the trend were identified as true cycles when they repeated more than twice. When the periods repeated just more than once within the dataset, we considered them as possible cycles.

2.2. On the origin of the long-term changes

For the long-period RS CVn system HK Lac we have a nearly 30 years long photoelectric database (Oláh et al. 1997). We used these data and the two-spot modelling results from Oláh et al. (1997) to separate the individual parameters contributing

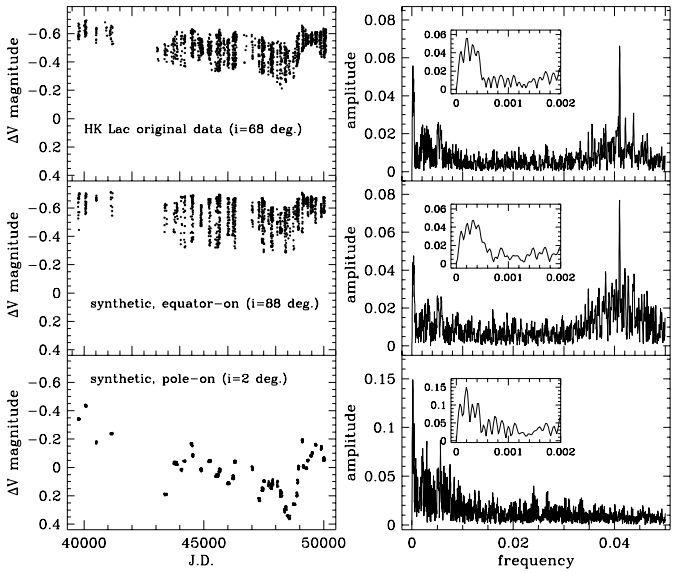

Fig. 1. Observed and artificial datasets (left column) of HK Lac and their respective amplitude spectra (right column). The synthetic data are generated for very high (i=88°) and very low (i=2°) inclinations and are displayed on the same magnitude scale. The inserts show an enlargement of the low-frequency part of the Fourier spectrum. For comparison, the rotational frequency is at 0.041 c/d.

to the light curve, i.e. the inclination of the rotational axis, the overall spot area, and the spot pattern as a function of time. The artificial datasets were created from the original Julian dates of the observations, thus keeping the time distribution of the artificial data the same as for the observations.

The detectability of the long-term changes depends on the inclination of the stellar rotation axis. This is shown in Fig. 1. The inclination for the artificial data was set to 88° and 2°resulting in two long-term light curves as if the star was seen pole-on or equator-on, respectively (Fig. 1, left column). As expected, long-term changes are more visible at low inclinations. The resulting amplitude spectra for the artificial HK Lac data are displayed in Fig. 1, right column, which shows that for low inclinations the amplitude of the long-term variation becomes larger and the amplitude of the rotational modulation becomes smaller. Quite the opposite behaviour is found for the high-inclination case.

Next, we generated synthetic datasets keeping either latitudes, longitudes, or size of the spots fixed at the average values while the other two of the three parameters were varied according to the individual light-curve fits. The period analysis of the synthetic data with fixed coordinates (longitudes or latitudes) showed that the low-frequency peaks in the amplitude spectra were very similar to that obtained from the original dataset (Fig. 2a–c). But when the sizes of the spots were fixed at the average values the low-frequency peaks basically disappeared (Fig. 2d). The amplitude spectrum from the total spot coverage showed a similar low-frequency pattern as the original dataset (Fig. 2e).

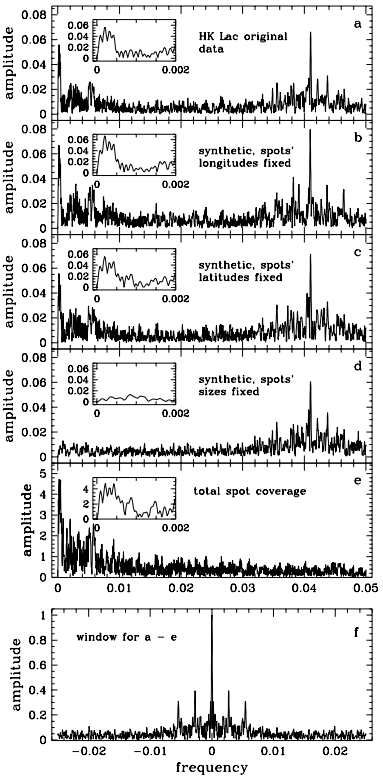

Fig. 2a – f. Test recovery of low-frequency light variations from artificial data for HK Lac. The top panel **a** shows again the amplitude spectrum from the original observations. Panels **b**, **c**, and **d** show the amplitude spectra of the synthetic data with fixed spot longitudes, spot latitudes, and spot sizes, respectively. Panel **e** shows the amplitude spectrum from the total spot coverage. The inserts again emphasize the low-frequency part of the spectra. Panel **f** is the window function.

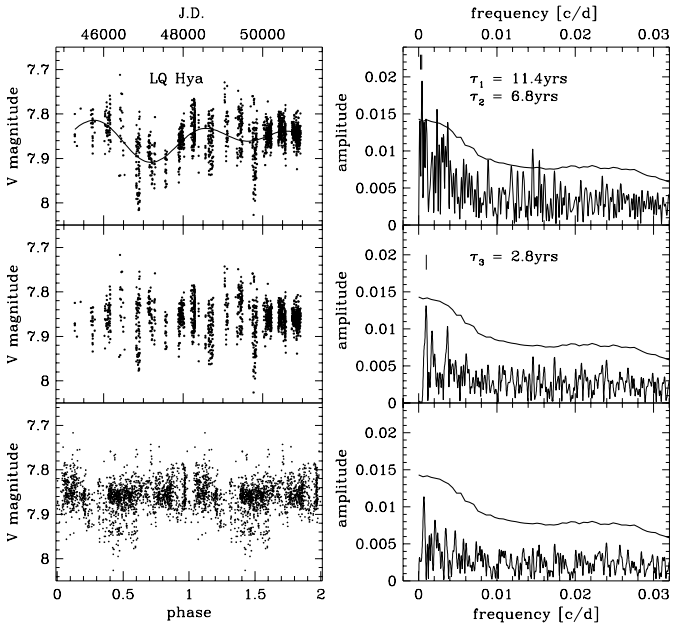

Fig. 3. LQ Hya. Top panels: the original observations and the fit with two periods (left) and the amplitude spectrum (right). Bars mark the periods. Middle panels: pre-whitened data with the two periods (left) and its new amplitude spectrum (right). A bar marks the third possible period. Lower panels: the pre-whitened magnitudes folded with the third period of 2.8 years (left), and the amplitude spectrum of the data further whitened with this third period (right). The continuous line represent the 3σ level of the last spectrum.

We should note that for the test star HK Lac Oláh et al. (1997) presumed high latitude spots to fit the observed light curves. The high latitude (polar) spot scenario for HK Lac, and also for many other stars, is supported using Doppler imaging results (Weber et al. 1999). Further support for the existence of polar spots comes from theoretical considerations (e.g. Schüssler 1996). On the other hand, from photometric spot modelling the information on spot latitudes remains limited (see Kővári & Bartus 1997), and latitude migration of spots cannot be determined.

Fig. 2 thus suggests that the shape and length of the observed long-term variability originates dominantly from the variability of the spot coverage and *not* from spot migrations.

3. Individual results

Table 1 summarizes the stars studied, their spectral types, and the orbital and rotational periods from the CABS II catalog (Strassmeier et al. 1993) if not stated otherwise in the text. Additionally listed are the non-empirical (NE) convective turnover time-scales ($\tau_c(NE)$) from Gunn et al. (1998) whenever available from their Table 2 (marked with an asterisk in our Table). Otherwise, it was interpolated using the empirical time scales τ_c(E) from Noyes et al.'s (1984) $(B-V)-\tau_c$ relationship and the average $B-V$ observed. The calculated Rossby numbers ($\mathrm{P_{rot}}/\tau_\mathrm{c}$) are tabulated as well. The results from our Fourier analysis are listed in three columns, τ_i (i=1,2,3), which denote the most significant resulting periods in decreasing lengths, and their respective light amplitudes. Colons mark those cycle lengths whose amplitude did not reach the 3σ level of the corresponding amplitude spectrum. Generally, the longest term variabilities are marked as τ_1, whereas τ_3 means the shortest possible cycle length found in the data. Note, however, that if only one cycle is found in the data that does not necessarily mean it is the shortest one. In these cases we decide whether they are the shortest- (τ_3) or the medium-long (τ_2) cycles on the basis of other considerations, see Sect. 4. The longest-term cycles (τ_1) are usually longer than our database, and we see only a long-term trend in the data beside the shorter variations. Finally, the length of the database studied is given in years.

The pre-whitened data from all the significant frequencies listed in Table 1 were again subjected to a Fourier analysis and a 3σ line was calculated from the resulting spectra for each star. This line is shown in the amplitude spectra in Figs. 3–12. A cycle length was considered real when the amplitude of the cycle frequency was above or close to the 3σ level.

The Fourier results for each star are discussed individually in the following subsections. No specific stellar details for our program stars are given, but some of the most comprehensive studies are cited. The interested reader may consult them for

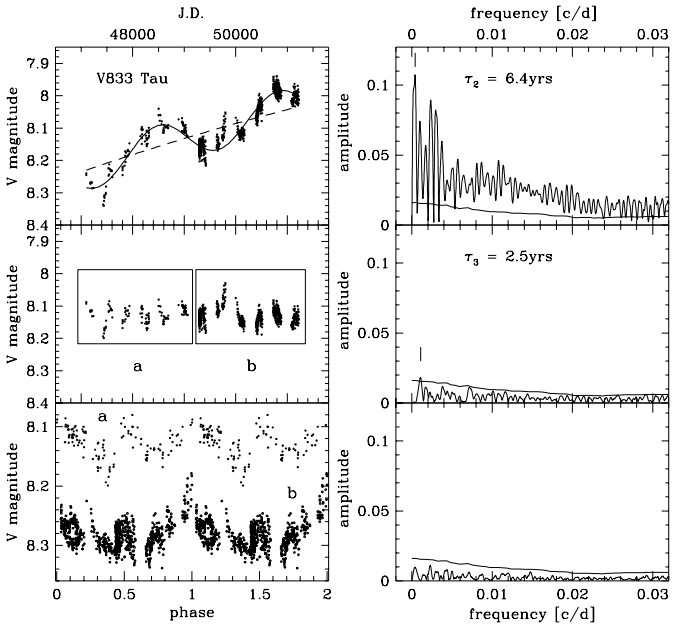

Fig. 4. V833 Tau. Top panels: the original observations fitted with a trend (dashed line) and one long period (left), and its amplitude spectrum (right). A bar marks the long period. Middle panels: pre-whitened data (left), and the amplitude spectrum from the pre-whitened data (right). A bar marks the second possible period. Lower panels: the pre-whitened magnitudes (separately from the two boxes in the middle left panel, data from box 'b' is shifted by 0.15 mag.) folded with the resulted second period of 2.5 years (left), and the amplitude spectrum of the data further whitened with this second period (right). The continuous line represents the 3σ level of the last spectrum.

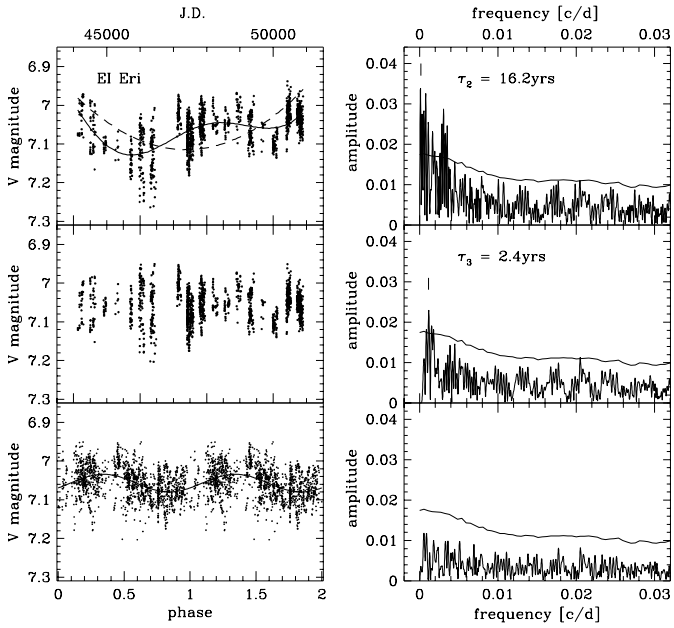

Fig. 5. EI Eri. Top panels: the original observations fitted with a trend (dashed line) and a 16-year period (left), and the amplitude spectrum (right). Middle panels: pre-whitened data (left) and the amplitude spectrum of the pre-whitened data (right). A bar marks the second possible period. Lower panels: the pre-whitened magnitudes folded with the second period of 2.4 years (left) and the amplitude spectrum of the data further whitened with this second period (right). The continuous line represents the 3σ level of the last spectrum.

further references or see the CABS II catalog (Strassmeier et al. 1993).

3.1. LQ Hya

LQ Hya is the only single star in our sample and is also the one with the shortest rotational period. Its light variability is monitored since 1982 (cf. SBCR 1997) and shows a fairly smooth change that can be approximated with two periods of 11.4 and 6.8 years. The shorter of these two periods has much higher power than the longer one and is close to the 7 years that has already been mentioned by SBCR (1997). A still shorter cycle of approximately 2.8 years may be present, but the folded light curve has too high scatter to be conclusive. The amplitude spectra, the observations and the fits, along with the residual magnitudes are displayed in Fig. 3.

3.2. V833 Tau

V833 Tau has the lowest inclination ($\approx 20°$) among the studied stars and its rotational modulation has therefore a comparably small amplitude. Even within an observing season the long-term variability can be on a larger scale than the rotational modulation itself. It is modulated with a period of about 6.4 years and, after pre-whitening the data, we obtain a possible second cycle length of 2.5 years. The latter one is quite uncertain and is better seen in the first half of the dataset (box 'a' in Fig. 4). The photographic observations (Bondar 1995) showed a cyclic sinusoidal light curve of the star with a period of around 60 years. The last maximum occurred in 1977 ($m_{pg} \approx B = 9\overset{\mathrm{m}}{.}09 \pm 0.02$, Bondar 1995; taking $B - V \approx 1\overset{\mathrm{m}}{.}1$ that corresponds to $V \approx 7\overset{\mathrm{m}}{.}99$), and by 1986-87 the star was again fainter by about $0\overset{\mathrm{m}}{.}3$–$0\overset{\mathrm{m}}{.}4$ but since then it started to brighten again. In 1998, V833 Tau was in its brightest state ever observed ($V \approx 7\overset{\mathrm{m}}{.}94$), which most likely means that the star was at its minimum activity ever observed. In a forthcoming paper (Oláh et al. 2000), we will model the entire light curves of V833 Tau with an appropriate spot model as a function of time. The amplitude spectra, the fit to the observations, and the residual magnitudes from the Fourier fits are displayed in Fig. 4.

3.3. EI Eri

EI Eri has now more than 18 years of photoelectric photometry. The first 16 years of observations were summarized by SBCR who found a possible 11 ± 1 year cycle. From the data available at that time, this value seemed to be real but the observations of the last two years contradict the 11-year cycle length. Berdyugina & Tuominen (1998) quote a 9 years long activity cycle on EI Eri from the positions of active regions. They do not discuss the change in the level of spottedness itself though. The long-term variability that is seen in the EI Eri magnitudes has a time-

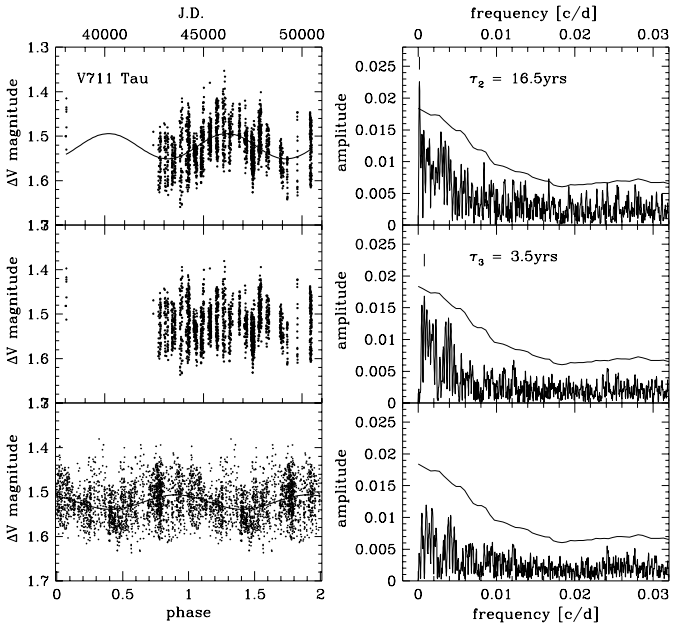

Fig. 6. V711Tau. Top panels: the original observations fitted with a period of 16.5 years (left) and the amplitude spectrum (right). Middle panels: pre-whitened data with the long period (left) and the amplitude spectrum of the pre-whitened data (right). Lower panels: the pre-whitened magnitudes folded with the second period of 3.5 years (left) and the amplitude spectrum of the data further whitened with this second period (right). The continuous line represents the 3σ level of the last spectrum.

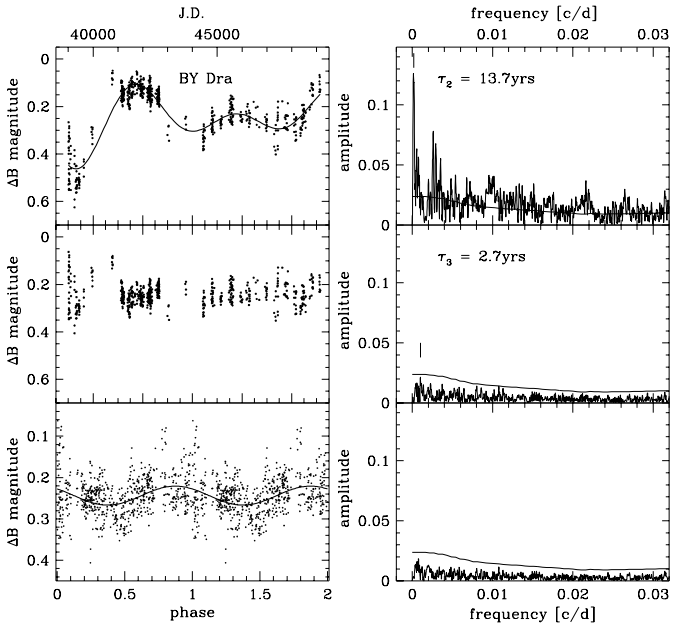

Fig. 7. BY Dra. Top panels: the original observations fitted with two close periods near 13.7 years (left) and the amplitude spectrum (right). Middle panels: pre-whitened data with the two close periods (left) and the amplitude spectrum of the pre-whitened data (right). A bar marks a possible third period. Lower panels: the pre-whitened magnitudes folded with the third period of 2.7 years (left) and the amplitude spectrum of the data further whitened with this third period (right). The continuous line represents the 3σ level of the last spectrum.

scale between $10 - 16$ years. The 16.2 years value we used is only a little less than the length of the database, depends on the trend that was subtracted and is thus very uncertain. After pre-whitening the data with a trend and a 16.2-year period, or any other combination of a trend and a long period between $10 - 16$ years, a significant period of 2.4 years remains in the data. The amplitude spectra, the fit to the observations and the residual magnitudes are displayed in Fig. 5.

3.4. V711 Tau

The photometric observations of V711 Tau were gathered from the literature and were supplemented with new data from Strassmeier & Bartus (1999). The database is now effectively 22 years long starting in 1975, but a few datapoints exist also from 1962–63. The Fourier analysis gave a 16.5 years long timescale of the variability that was also found by Strassmeier & Bartus (1999). Removing this sinusoidal wave from the data, a very weak short-term cycle with a period of 3.5 years remains. Vogt et al. (1999) found some evidence of an about 3 years long cycle in the total spotted area (polar spot and low latitude spots) using Doppler imaging from 11 years of observations. Whether this agreement is coincidental remains to be determined but clearly demonstrates the importance of long-term monitoring of this star. The rotational modulation has a large amplitude and shows up as large scatter in the folded long-term lightcurve. The amplitude spectra, the fit to the observations, and the residual magnitudes are displayed in Fig. 6.

3.5. BY Dra

The binary BY Dra consists of two active K-dwarf stars, where the primary makes up for about 2/3 of the light from the system. The orbit is rather eccentric ($e \approx 0.3$) but the rotation of the two components is pseudosynchronous to the orbital motion. The long-term spot activity of the individual components was discussed in detail by Kővári (1999) using two-colour photometry between 1965 to 1993. We used the ΔB data instead of ΔV as for the other targets in this paper because they span a longer baseline in time. BY Dra is also known to exhibit a very long-term sinusoidal variability with a period of 50–60 years (see Bondar 1995). Pettersen et al. (1992) found a cyclic behaviour on a 13–14 years long time scale in the O–C diagram from timings of the light-curve minima, and suggested a longitudinal shift of the dominant spotted region(s) of about 50° per year (or 0.4° per stellar rotation). Our Fourier analysis confirms the intermediate long-term variability and we find a time scale of 13.7 years. However, we could only fit the long-term variability with two closely-spaced periods (13.70000 and 13.69973 years) but can not offer a physical meaning of this result. The combination of the possibly different timescales of the spot area changes on the two components of BY Dra separately (found by Kővári 1999) could also produce such a long-term variability

Table 1. Basic stellar data and results

Star	spectral class	$P_{\rm orb}$	$P_{\rm rot}$	τ_c	Rossby no.	τ_1	Δm_1	τ_2	Δm_2	τ_3	Δm_3	time base
		(days)	(days)	(days)		(yrs)	(mag)	(yrs)	(mag)	(yrs)	(mag)	(yrs)
LQ Hya	K2V	single	1.6009	23.34	0.069	11.4	0.038	6.8	0.058	2.8:	0.017	15.6
V833 Tau	K5V	1.7880	1.7936	28.31*	0.063	trend (60?)	–	6.4	0.128	2.5	0.030	11.3
EI Eri	G5IV	1.9472	1.9527	19.32	0.099	trend	–	16.2	0.122	2.4	0.046	18.5
V711 Tau	G5IV+K1IV	2.8377	2.841	92.68*	0.031	–	–	16.5	0.056	3.5:	0.032	22.0
BY Dra	K4V+K7.5V	5.7951	3.8285	32.29	0.119	trend (55?)	–	13.7**	–	2.7:	0.046	27.8
HU Vir	K0III-IV	10.3876	10.42	79.43*	0.131	trend	–	–	–	5.6**	–	16.0
IL Hya	K0III-IV	12.908	12.791	107.90*	0.119	trend	–	13.0	0.151	–	–	27.3
VY Ari	K3-4IV-V	13.198	16.199	67.76	0.239	–	–	15.3	0.156	–	–	22.2
HK Lac	K0III	24.4284	24.378	90.57*	0.269	$\geq$34.2	–	13.0	0.040	6.8	0.069	30.3
IM Peg	K2III	24.6488	24.494	43.75*	0.560	$\geq$48.3	–	–	–	–	–	27.2

* non-empirical values from Gunn et al. (1998)
** two close periods; no amplitude can be given

Table 2. Additional stars with long periods

Star	Spectral type	P_{orb} (days)	P_{rot} (days)	τ_1 (years)	τ_2 (years)	τ_3 (years)	Rossby no.	Reference
XY UMa	G3V/[K4-5V]	0.4790	0.479	30			0.024	Henry et al. (1995) and refs. therein
AB Dor	K0-K2 IV-V	single*	0.514		5.3		0.024	Amado et al. (2000)
CG Cyg	G9.5V/K3V	0.6311	0.631	41			0.028	Henry et al. (1995) and refs. therein
WY Cnc	G5V/[M2]	0.8294	0.829		10.0		0.063	Henry et al. (1995) and refs. therein
CC Eri	K7Ve/dM4	1.5615	1.561	55			0.042	Henry et al. (1995) and refs. therein
AR Lac	G2IV/K0IV	1.9832	1.983		17.0		0.081	Lanza & Rodonò (1999a)
RS CVn	F4IV/G9IV	4.7979	4.791		20.0		0.078	Lanza & Rodonò (1999a)
DX Leo	K0V	single	5.377			3.89	0.283	Messina et al. (1999)
UX Ari	G5V/K0IV	6.4379	6.438		10.0		0.114	Henry et al. (1995) and refs. therein
II Peg	K2-3 V-IV	6.7242	6.718		11.0	4.4	0.091	Henry et al. (1995) and refs. therein
SS Boo	G0V/K0IV	7.6061	7.606		11.5		0.119	Henry et al. (1995) and refs. therein
σ Gem	K1III	19.6045	19.410			8.5	0.308	Henry et al. (1995) and refs. therein
λ And	G8IV-III	20.5212	53.952			11.1	0.682	Henry et al. (1995) and refs. therein

*distant companions, see Guirado et al. (1997)

that we observed. The 50–60 years long cycle (Bondar 1995) did not show up in our data. After pre-whitening the data, a very weak and possibly spurious short-term cycle of about 2.7 years remained. The amplitude spectra, the fit to the observations, and the residual magnitudes are displayed in Fig. 7.

3.6. HU Vir

The light variation of HU Vir was discovered in the early 1980's but for a few years only sparse observations were gathered. Most of the data were reported by SBCR who observed HU Vir regularly from 1991 onwards. SBCR also reported a possible 4–5 years cyclic variation in the mean brightness that is confirmed from our Fourier analysis with two more years of observations. A 5.6-years period (and its aliases) seems to be the only peak in the amplitude spectrum above the 3-σ line (Fig. 8). As in the case of BY Dra, the long-term modulation was fitted best with two closley-spaced periods because of a variable amplitude of the 5.6 years cycle. If we leave away the first (or the first two) seasons of data in the analysis – which make up for the long time coverage (see Fig. 8) – we still obtain a 5.4 years cycle, which strenghtens our initial result. Apart from the 5.6 years cycle, no significant variation is found in the data except, of course, the rotational modulation. We note that, as recently discovered by Fekel et al. (1999), HU Vir is a member of a spectroscopic triple system with an orbital period of about 6.1 years. The dataset and amplitude spectra for this star are shown in Fig. 8.

3.7. IL Hya

The photometric history of the K0-giant active binary IL Hya is summarized by SBCR until 1996. A more detailed discussion on the properties of the system is given by Weber & Strassmeier (1998) and on the orbital aspects by Fekel et al. (1999). The Fourier spectrum of the long-term variabiliy of this star is simple and is dominated by a continuous brightening since the discovery of its light variations in 1971. Superimposed on it is a cycle of about 13 years in length. After prewhitening the data

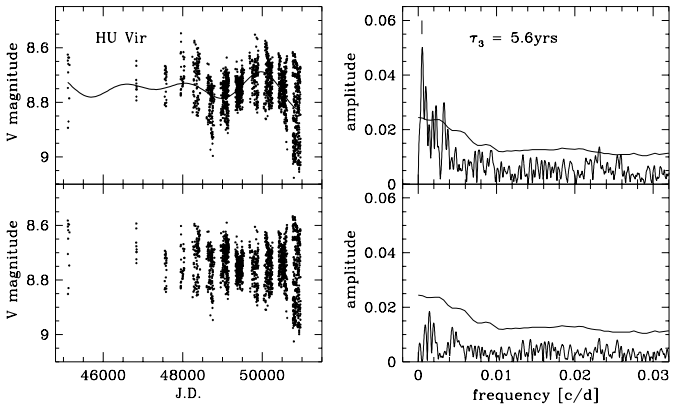

Fig. 8. HU Vir. Top panels: the original observations fitted with two close periods around 5.6 years (left) and the amplitude spectrum (right). Bottom panels: pre-whitened data with the two close periods (left) and the amplitude spectrum of the pre-whitened data (right). No further significant period is found. The continuous line represents the 3σ level of the last spectrum.

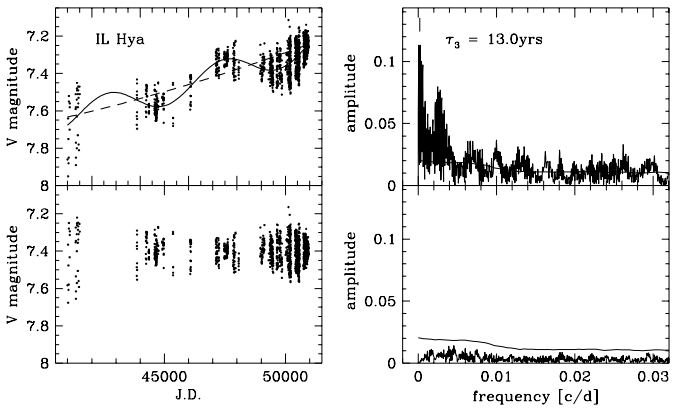

Fig. 9. IL Hya. Top panels: the original observations fitted with a trend (dashed line) and a long period of 13 years (left) and the amplitude spectrum (right). Bottom panels: pre-whitened data with the trend (dashed line) and the long period (left), and the amplitude spectrum of the pre-whitened data (right). Again, the continuous line represents the 3σ level of the last spectrum.

with the trend and the cycle, only white noise remains in the low-frequency part of the amplitude spectrum (Fig. 9).

3.8. VY Ari

VY Ari is a very active and the only asynchronously rotating star in our sample. Strassmeier & Bopp (1992) summarized and discussed the existing photometric data of the star between 1974–1991. There is a gap of ten years in the photometric coverage but despite a long-term variability is indicated by the data. SBCR already estimated a possible cycle length of ≈14 years that agrees well with our determination of 15.2 years (Fig. 10).

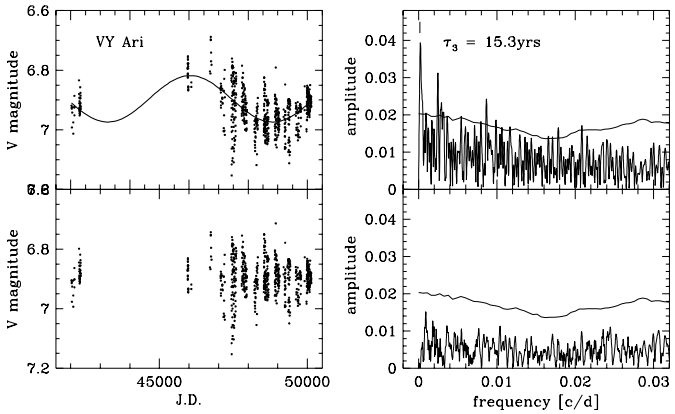

Fig. 10. VY Ari. Top panels: the original observations fitted with a period of 15.2 years (left), and the amplitude spectrum (right) Bottom panels: pre-whitened data with the long period (left) and the amplitude spectrum of the pre-whitened data (right). No further significant period was found. The continuous line represents the 3σ level of the last spectrum.

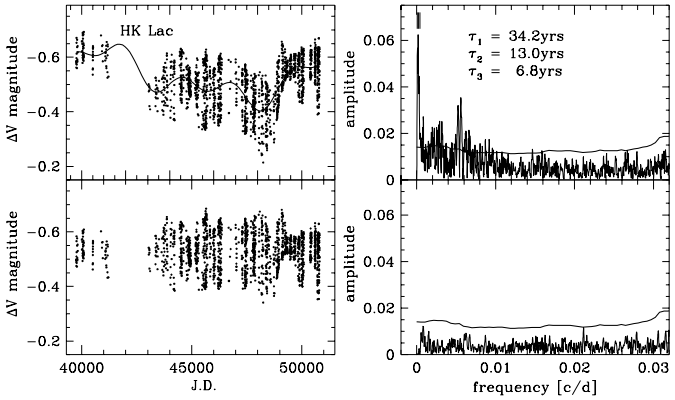

Fig. 11. HK Lac. Top panels: the original observations fitted with three periods (left) and the amplitude spectrum (right). Vertical bars mark the long periods. Bottom panels: pre-whitened data with the three long periods (left) and the amplitude spectrum of the pre-whitened data (right). A close-up of the low-frequency region is shown in Fig. 1 (top panels). The continuous line represents the 3σ level of the last spectrum.

3.9. HK Lac

Thirty years of photometry of HK Lac was recently discussed by Oláh et al. (1997). The observations used in that paper are now supplemented with two more years of data. The Fourier analysis of the present dataset reconstructed three long time-scale variations. The longest one, 34.2 years, is approximately the length of the dataset itself and is statistically not significant, though visual inspection of the light curve in Fig. 11 shows that some variation on a time-scale of a few tens of years must be present. The 13.0 years and 6.8 years periods probably are real. Especially interesting is the 6.8 years cycle. In an earlier paper by Oláh et al. (1991) the lifetime of the activity centers of HK Lac was found to be close to 7 years using the results from detailed spot modelling. Furthermore, Oláh et al. (1997) found discontinuities in the distribution of rotational phases of activity

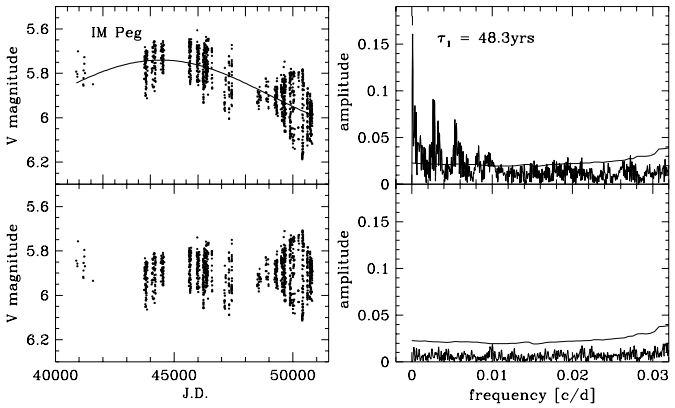

Fig. 12. IM Peg. Top panels: the original observations fitted with a long period of 48.3 years (left) and the amplitude spectrum (right). Bottom panels: pre-whitened data period (left), and the amplitude spectrum of the pre-whitened data (right) showing only noise. The continuous line in the frequency plots represents the 3σ level.

centers on the same time-scale (for both results see Fig. 8 of Oláh et al. 1997).

3.10. IM Peg

IM Peg is the longest period star in our sample. SBCR gave a summary of its photometric observations. Its spectral type was recently revised to K2III by Berdyugina et al. (1999). Supplemented with two more years of photometric data, we analysed the 27 year of photometry from SBCR that has evidently a secular variation. We obtained 48.3 years as the long period with the highest peak but note that it is twice as long as the time coverage of the data (Fig. 12). However, no other cycle-like variability is present in the data after pre-whitening with the 48.3 years long "period". The remaining white noise in the periodogram verifies that, if any cyclic variability exists on IM Peg, it has a time-scale longer than about half a century.

4. Discussion

The results of our period analysis of ten rapidly-rotating active stars are summarized in Table 1. We derived double and multiple time-scale variabilities for six of the ten stars and for three stars we found one-one cycle.

From the literature, we gathered further cycle lengths or variability time-scales for thirteen additional stars: λ And, UX Ari, SS Boo, WY Cnc, CG Cyg, CC Eri, σ Gem, II Peg and XY UMa (from Henry et al. 1995, and references therein); RS CVn and AR Lac (from Lanza & Rodonò 1999a), DX Leo (from Messina et al. 1999) and for AB Dor (from Amado et al. 2000). Table 2 is a summary of the relevant data. Only the variabilities in the overall brightness of the stars were considered. We list the shortest cycle lengths as τ_3, τ_2 gives those periods that resemble the medium-term variability and τ_1 are the longest-term variations.

Fig. 13 summarizes our results in a $\log - \log$ presentation of normalized cycle periods versus inverse rotation periods. First,

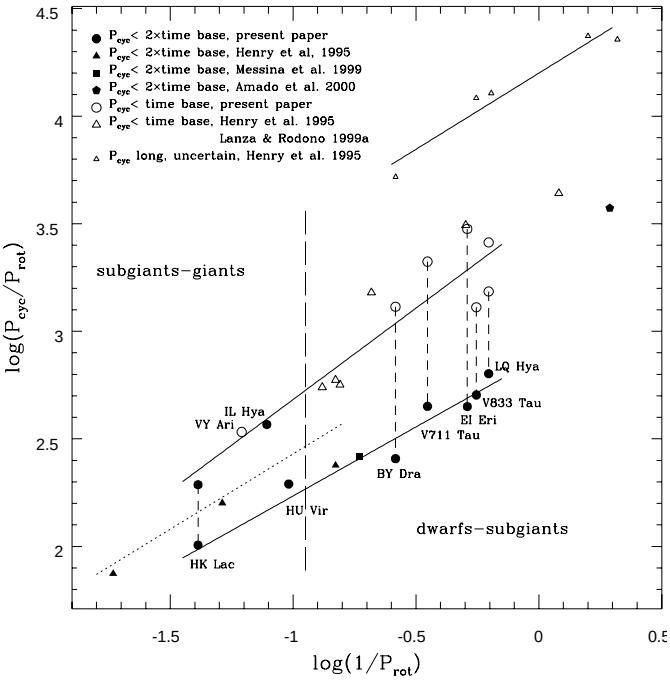

Fig. 13. Variation of $P_{\rm cyc}/P_{\rm rot}$ vs. $1/P_{\rm rot}$ in logarithmic scale. The vertical long-dashed line separates the stars above and below a rotational period of 10 days. Solid lines represent linear least-squares approximations to the data for the six stars of our sample with double cycles that are connected with dashed lines, and to the longest cycles found in the literature (upper right corner) (c.f. Tables 1 and 2). The dotted line is from Baliunas et al. (1996). See text.

the fits for the shortest- and the medium-long cycles were made using only the six double cycles determined by us. The rest of the cycles found by us and from the literature clearly fall in or close to either of the two branches, this way we can decide if the given cycle is the shortest possible one (τ_3) or a medium-long one (τ_2). These fits are plotted in Fig. 13. Next, we made new fits for all the cycles that seem to represent the two branches. The slope of the trend between $\log(P_{\rm cyc}/P_{\rm rot})$ and $\log(1/P_{\rm rot})$ for the shortest cycles is 0.57$\pm$0.04 (0.64$\pm$0.07) with a correlation coefficient of 0.98 (0.98), in brackets are the results we got using only our six double cycles. For the longer, less certain cycles it is 0.83$\pm$0.08 (0.85$\pm$0.19) with a correlation coefficient of 0.94 (0.91). The five longest cycle lengths (found in the literature) yield 0.71 ± 0.10 with a correlation coefficient of 0.97. For the dwarfs-subgiants regime the shortest and the longer possible cycles are well separated. A similarly well-established separation is not present for the subgiants-giants regime, that has only five stars (VY Ari, a relatively slowly rotating dwarf-subgiant star falls also to this regime), also, the giants form a physically more inhomogeneous group than the dwarf stars.

The resulted slopes agree with the slope of 0.74 for slowly rotating main sequence stars (Baliunas et al. 1996). Note that Baliunas et al. (1996) use H&K emission-line flux as activity indicator compared to visual brightness as in our case. Nevertheless, we may plot the results from Baliunas et al. (1996) as a dotted line in Fig. 13 where they appear with $\log(1/P_{\rm rot})$ of up to

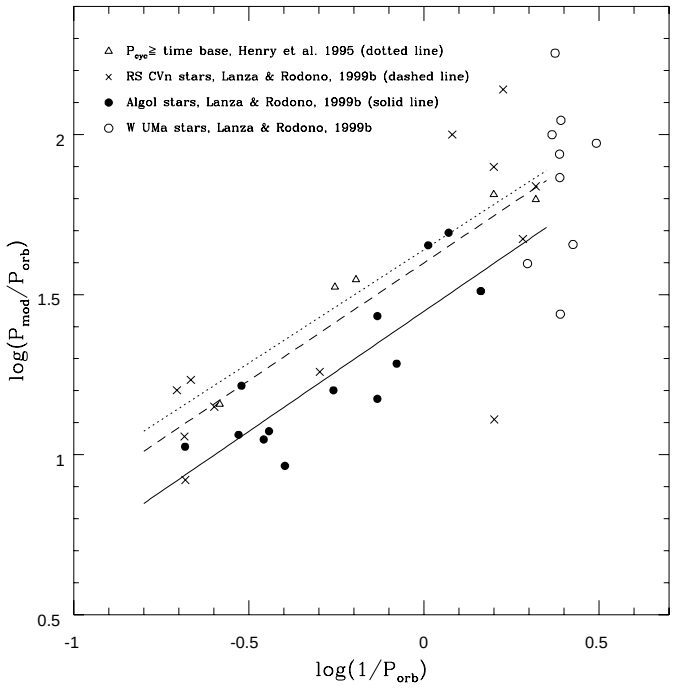

Fig. 14. Variation of $P_{\rm mod}/P_{\rm orb}$ vs. $1/P_{\rm orb}$ in logarithmic scale using cycles from orbital period variations. Triangles are the same five stars as in the upper right region of Fig. 13. Lines represent linear least-squares approximations to the data. See text.

approximately -0.8 corresponding to the fastest rotators in their sample. The similarity of the trends for the different groups of stars (fast rotating dwarfs-subgiants-giants and slowly rotating lower main-sequence stars) suggests that the ratio of $P_{\rm cyc}/P_{\rm rot}$ has a physical meaning and that it may provide a link between the observational and theoretical studies of stellar dynamos, as has already been suggested by Soon et al. (1993).

All of the five short-period, main-sequence stars studied have double-cyclic behaviour and two of them, V833 Tau and BY Dra, may have long-term variability on even three timescales. It is possible that the shortest cycles are not always observable or are not always present. We note that for five main-sequence stars, Baliunas et al. (1996) also found double-cycle periods. The Sun shows cyclic variability of its overall activity on at least three time scales. Beside the ≈11 years long spot cycle, the solar activity has an about 80-year periodicity (the so-called Gleissberg cycle) and an even longer term (200–300 years) pseudo-cycle (Wolf, Spörer, Maunder minima). See, e.g., the proceedings edited by Sonett et al. (1991). A medium long-term cycle length of the Sun was detected by Pulkkinen et al. (1999), who found an ≈90 years long cyclic variation of the 'magnetic equator' of the Sun between the sourthern and northern latitudes, that was strongly resembling to the Gleissberg cycle. It is worth to note that the time-scale of the long-term variabilities on BY Dra and V833 Tau are 5–10 times shorter and their rotational periods are 7-15 times shorter than on the Sun.

A connection between cyclic orbital-period variations or active-longitude changes and the overall brightness change is very likely (see the results for HK Lac in Sect. 3.9). A full theory that connects all these phenomena is still missing. A link between orbital-period variation and stellar luminosity was proposed by Applegate (1992) and further discussed by Lanza et al. (1998) and possibly verified for CG Cyg by Hall (1991). The main agent is the change of the gravitational quadrupole moment due to a periodic dredge up of high angular momentum as a function of the stellar magnetic cycle. Lanza et al. (1998) proposed a periodic change of the azimuthal field component from an $\alpha^2\Omega$ dynamo that would cause varying influence of the Lorentz force on the convective envelope, and thus also a change of the oblateness and the gravitational quadrupole moment.

Orbital-period variations of Algols, RS CVn binaries and W UMa stars were recently summarized by Lanza & Rodonò (1999b). Using the orbital periods and their periodic variations (modulations) listed in that paper we plot $\log(P_{\rm mod}/P_{\rm orb})$ vs. $\log(1/P_{\rm orb})$ in Fig. 14 and compare them with the five stars from Henry et al. (1995) from the upper right corner of Fig. 13. The W UMa stars do not show any trend but a correlation is seen for Algols and RS CVn stars. This relation is similar to the one we found between rotational periods and photometric cycles for our sample of fast rotating active stars (see Fig. 13). The slopes of the trends between $\log(P_{\rm mod}/P_{\rm orb})$ and $\log(1/P_{\rm orb})$ for the RS CVn stars and the Algols are 0.74±0.19 and 0.75±0.13, respectively, and their correlation coefficients are 0.78 and 0.86, respectively. The five stars with the longest cycles from the photometry result in a slope of 0.71±0.10 with a correlation coefficient of 0.97 (as mentioned above), but this value is uncertain because of the small number of the fitted points. The eccentricity of the orbits of most Algols and RS CVns is small and their rotation is synchronized to the orbital motion. Therefore, the orbital periods are close to the rotational periods and we have similar correlations between, firstly, the rotational periods and the long-term photometric variabilities and, secondly, the orbital (≈ rotational) periods and the orbital-period variations.

A plot of the log inverse Rossby number and $\log(\omega_{cyc}/\Omega)$ for our program stars, supplemented with thirteen additional stars from the literature (Table 2) is displayed in Fig. 15 together with the active stars (Wilson sample), BY Dra stars and RS CVn stars from Saar and Brandenburg (1999, hereafter and in Fig. 15 S&B). (We did not take into account the W UMa, dwarf nova, nova, nova-like and pulsar secondary stars from S&B since we wanted to use similar stars to our sample.) We use the parametrization of S&B that allows a direct comparison with their results of cycle periods for active stars. S&B's active (A) and superactive (S) branches are also plotted with dashed lines, a fit to the transitional regime stars of Fig. 5. of S&B are also drawn with a dashed line (Saar, private communication). The small symbols represent less certain data from our sample and from S&B.

In Fig. 15 big dots and cirles represent the values calculated using the shortest possible cycle lengths that repeated more than twice during the observations from the present analysis for LQ Hya, V833 Tau, EI Eri, V711 Tau, BY Dra, HU Vir, IL Hya and HK Lac, and also represent four additional stars from the literature with similarly well established cycle lengths: σ Gem,

Table 3. Cycle lengths from different sources

Star	Cycle length (years) this paper	other source	Method/activity tracer	Reference
BY Dra	13.7	13−14	O−C of times of minima	Pettersen et al. (1992)
V711 Tau	3.5	≈ 3	Doppler imaging, total spot area	Vogt et al. (1999)
	16.5	18	orbital period fluctuations	Donati (1999)
HU Vir	5.6	6.1	orbital period of the triple system	Fekel et al. (1999)
HK Lac	6.8	≈ 7	discontinuities of spot phases	Oláh et al. (1997)
EI Eri	10-16/2.4	9.0	alternating minima changes	Berdyugina & Tuominen (1998)
IM Peg	≥ 48	20.5	alternating minima changes	Berdyugina et al. (1999)

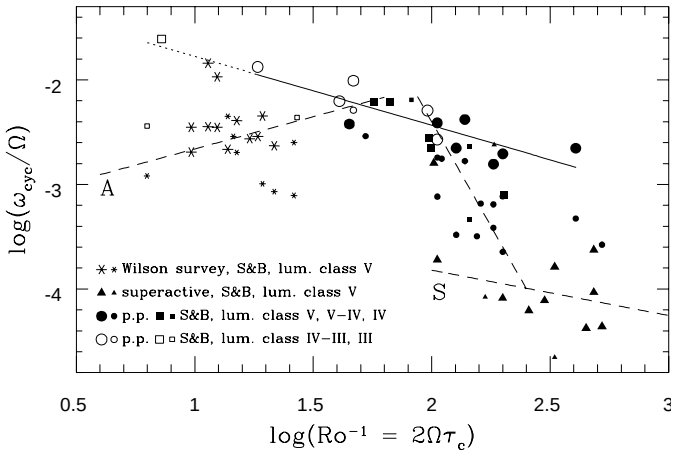

Fig. 15. A plot of the log inverse Rossby numbers vs. log(ω_{cyc}/Ω) for the stars from the present paper and for active stars (Wilson sample), BY Dra stars and RS CVn stars from S&B. Big and small symbols represent more and less certain cycles. A and S branches plotted with dashed lines are from S&B, also plotted with dashed line is a fit for the transitional regime of S&B (Saar, private comm.). The solid line (continued with dotted line) is a fit using the shortest cycles lengths found in the present paper (round symbols). See text.

II Peg and λ And from Henry et al. (1995) and DX Leo from Messina et al. (1999). For the shortest cycle lengths we find a trend between log(Ro^{-1}) and log(ω_{cyc}/Ω) with a slope of -0.66 ± 0.13 with a correlation coefficient of 0.85 that is plotted with a straight line that we continue as dotted line outside the range of our data. Nine stars with well determined cycles from S&B lie at or close to our relation, and two of them are double-cycle stars from Wilson's sample.

According to our results (and also found e.g. by Saar & Baliunas 1992) the presence of multiple cycles could be a common feature of active stars. The relation between log(Ro^{-1}) and log(ω_{cyc}/Ω) has different branches, first demonstrated by Saar and Baliunas (1992). Comparing Fig. 15 with Fig. 5 of S&B we find that the relation found from the shortest cycle lengths that were determined in the present paper lie paralel and well above the values and relation determined by S&B for the S-branch stars. The other, less certain cycles found by us or in the literature (marked with smaller symbols) seem to scatter between our relation and the S-branch. S&B's relation for S stars runs closest to the longest observed cycle lengths. The relation for A stars, that are determined mostly by the Wilson sample stars, has an opposite slope. However, the Wilson sample consists of slowly rotating single, solar type stars, whereas the other stars (from the present paper and from S&B) are fast rotators, and the vast majority of them is a member of a binary system that means a physical difference. Still, the shorter cycles of the two double-period stars of the Wilson sample we plotted agree well with the continuation of our relation for the shortest cycles lengths. Looking at Fig. 15 we may speculate, that our relation for the shortest and S&B's relation for the longest cycles (S-branch) could define an area where the limits follow from the possible shortest and longest cycle lengths for given rotational periods and Rossby numbers of active stars, and the values determined by medium-long cycle lengths fall into this area.

In Table 3, we summarize the cycles of six particular systems found in this paper, together with reliable cycle-length values of the same stars, but derived by other methods. For BY Dra and HK Lac, the phases of the spots and the spot-area changes show similar cyclic behaviour. In case of V711 Tau, the shortest cycle length of the spottedness found by us is supported by Doppler-imaging results, and the medium-long cycle length is similar to the cycle length found from orbital period fluctuations. Finally, the long orbital period of the recently discovered triple system HU Vir is closely resembling the photometric cycle length. Table 3 thus suggests some relationship between the various types of stellar cycles that may lead us to a more complex picture of stellar activity.

5. Conclusions

- From 11–30 years of photometric data of ten rapidly-rotating active stars, we performed Fourier analyses with emphasis on long periods or quasi periods (trends). We determined cycle lengths for nine of the ten stars studied and for six of those double or multiple time-scale variations were found.
- The long-term brightness variations of active stars are governed by a change of their overall spot coverage. Spot migration does not affect the shape nor the length of the cycles observed.
- A correlation between cycle length (from brightness variations) and stellar rotational period seems evident. Cycles are generally longer for slower rotators. Relations exist between the shortest possible cycle and the rotational period

as well as for the longer cycle and the rotational period, that is well separated for dwarf stars.
- The value ω_{cyc}/Ω calculated from well-determined shortest-cycle lengths possibly correlate with the inverse Rossby numbers of the stars investigated. At the moment, correlations for multiple cycles is hampered by our relatively small sample, short observing time-base, and by uncertainties in computing Rossby numbers of giant stars.
- Several of the cycle lengths determined from brightness variations agree with cycle lengths from other activity tracers or found with other methods.

Acknowledgements. Our sincere thanks are due to Drs. J. Jurcsik, Zs. Kővári, A. Lanza and S. Saar for their critical remarks and helpful discussions. We appreciate very much the kind assistance of J. Bartus in the data handling. An anonymous referee's questions helped to improve the discussion substantially. Financial supports from the Hungarian government through OTKA T-026165, T-032846, and AKP 97-58 2,2 are acknowledged. KGS appreciates support from the Austrian Science Foundation (FWF) grants S7301-AST and S7302-AST.

References

Amado P.J., Cutispoto G., Lanza A., Rodonò M., 2000, In: *Proc. 11th Cambridge Workshop on Cool Stars, Stellar Systems and the Sun*
Applegate J.H., 1992, ApJ 385, 621
Baliunas S.L., Nesme-Ribes E., Sokoloff D., Soon W.H., 1996, ApJ 460, 848
Berdyugina S.V., Tuominen I., 1998, A&A 336, L25
Berdyugina S.V., Ilyin I., Tuominen I., 1999, A&A, in press
Bondar, N.I., 1995, A&AS 111, 259
Donati J.-F., 1999, MNRAS 302, 457
Fekel F.C., Strassmeier K.G., Weber M., Washuettl A., 1999, A&AS 137, 369
Guirado J.C., Reynolds J.E., Lestrade J.-F., et al. 1997, ApJ 490, 835
Gunn A.G., Mitrou C.K., Doyle J.G., 1998, MNRAS 296, 150
Hall D.S. 1991, ApJ 380, L85
Hartmann L., Bopp B.W., Dussault M., Noah P.V., Klimke A., 1981, ApJ 249, 662
Henry G.W., Eaton J.A., Hamer J., 1995, ApJS 97, 513
Kolláth Z., 1990, *The program package MUFRAN*, Occasional Technical Notes of Konkoly Observatory, No. 1 (www.konkoly.hu/Mitteilungen/Mitteilungen.html#TechNotes)
Kővári Zs., 1999, In: Butler C.J., Doyle J.G. (eds.) *Solar and Stellar Activity: Similarities and Differences*, PASPC 158, p. 166
Kővári Zs., Bartus J., 1997, A&A, 323, 801
Lanza A.F., Rodonò, M., 1999a, In: Butler C.J., Doyle J.G. (eds.) *Solar and Stellar Activity: Similarities and Differences*, PASPC 158, p. 121
Lanza A.F., Rodonò, M., 1999b, A&A 349, 887
Lanza A.F., Rodonò, M., Rosner R., 1998, MNRAS 296, 893
Massi M, Neidhöfer J., Torricelli-Ciamponi G., Chiuderi-Drago F., 1998, A&A 332, 149
Messina S., Guinan E.F., Lanza A.F., Ambruster C., 1999, A&A 347, 249
Noyes R.W., Hartmann L.W., Baliunas S.L., Duncan D.K., Vaughan A.H., 1984, ApJ, 279, 763
Oláh K., Kolláth Z., 1999, In: Butler C.J., Doyle J.G. (eds.) *Solar and Stellar Activity: Similarities and Differences*, PASPC 158, p. 174
Oláh K., Hall D.S., Henry G.W., 1991, A&A 251, 531
Oláh K., Kővári Zs., Bartus J., et al., 1997, A&A, 321, 811
Oláh K., Strassmeier K.G., Kővári Zs., et al., 2000, A&A, in preparation
Pettersen B.R., Oláh K., Sandmann W.H., 1992, A&AS 96, 497
Phillips M. J., Hartmann L., 1978, ApJ 224, 182
Pulkkinen P.J., Brooke J., Pelt J., Tuominen I., 1999, A&A 341, L43
Radick R.R., Lockwood G.W., Skiff B.A., Baliunas S.L., 1998, ApJS 118, 239
Roberts D.H., Lehar J., Dreher J.W., 1984, AJ 93, 968
Saar S., Baliunas S.L. 1992, In: Harvey K.L. (ed.) *The Solar Cycle*, ASP Conf. Ser. Vol. 27, p. 150
Saar S.H., Brandenburg A., 1999, ApJ 524, 295 (S&B)
Soon W.H., Baliunas S.L., Zhang Q., 1993, ApJ 414, L33
Schüssler M. 1996, In: Strassmeier K.G., Linsky J.L. (eds.) *Stellar Surface Structure*, Proc. IAU Symp. No. 176, Kluwer Acad. Publishers, p. 269
Sonett C.P., Giampapa M.S., Matthews M.S. (eds.), 1991, *The Sun in Time*, The Univ. of Arizona Press, Tucson
Strassmeier K.G., Bartus J., 2000, A&A 354, 537
Strassmeier K.G., Bopp B.W., 1992, A&A 259, 183
Strassmeier K.G., Hall D.S., Fekel F.C., Scheck M., 1993, A&AS 100, 173
Strassmeier K.G., Bartus J., Cutispoto G., Rodonó M., 1997, A&AS 125, 11 (SBCR)
Vogt S.S., Hatzes A., Misch A.A., Kürster M., 1999, ApJS 121, 547
Weber M., Strassmeier K.G., 1998, A&A 330, 1029
Weber M., Washuettl A., Strassmeier K.G., 1999, In: Pallavicini R. (ed.) *Stellar clusters and associations: rotation, convection and dynamos*, Palermo, PASPC, in press
Wilson O.C., 1978, ApJ 226, 379